BILINGUAL PUBLISHING GROUP

Journal of Environmental & Earth Sciences

https://journals.bilpubgroup.com/index.php/jees

ARTICLE

Controls on Faulted Sub-Depression Patterns in Continental Rifted Basins: The Beier Depression, Hailar Basin, Northeastern China

Fangju Chen [1,2], Ya Tian [1,2], Gang Li [3*], Yougong Wang [3], Huaye Liu [1,2], Yue Zou [1,2], Mengxia Li [1,2]

[1] *State Key Laboratory of Continental Shale Oil, Daqing 163712, China*

[2] *Exploration and Development Research Institute of PetroChina Daqing Oilfield Company Limited, Daqing 163712, China*

[3] *Sanya Offshore Oil & Gas Research Institute, Northeast Petroleum University, Sanya 572025, China*

ABSTRACT

In contrast to well-studied rift basins in NE China, the Hailar Basin has received relatively less attention regarding the combined patterns of different types of grabens and half-grabens. This study aims to explore whether the combined patterns of grabens in the Hailar Basin exhibit similar characteristics to those in other NE China rift basins and to identify the underlying causes. To achieve this, a comprehensive analysis of the major fault systems and the combined patterns of faulted sub-depressions, as well as their controlling mechanisms, was conducted. This analysis utilized the latest 3D seismic data that cover nearly the entire Beier Depression. Three groups of pre-existing fault systems were observed in the basement of the Beier Depression, and they are the NEE-EW-trending fault systems, the NE-trending fault systems, and the NW-trending fault systems. The NEE-EW-trending fault systems were distributed in the central part of the Beier Depression and primarily controlled the sedimentary filling of the Tongbomiao and the Lower Nantun Formations. The NE-trending fault systems were distributed in the southwestern part of the Beier Depression and primarily controlled the sedimentary filling of the Upper Nantun Formations. The NW-trending fault systems were distributed rarely in the Beier Depression. Five kinds of combined patterns of the sub-depressions were developed in the Beier Depression, and they are the parallel, en echelon, face-to-face, back-to-back, and S-shaped combined patterns. They were controlled by the NEE-EW-trending and the NE-trending fault systems with different orientations, arrangements, and activation sequences.

Keywords: NE China; Hailar Basin; Beier Depression; Combined Pattern of Sub-Depressions; Continental Rift Basin

*CORRESPONDING AUTHOR:

Gang Li, Sanya Offshore Oil & Gas Research Institute, Northeast Petroleum University, Sanya 572025, China; Email: ligangcug@163.com

ARTICLE INFO

Received: 23 January 2025 | Revised: 21 February 2025 | Accepted: 26 February 2025 | Published Online: 6 May 2025
DOI: https://doi.org/10.30564/jees.v7i5.8543

CITATION

Chen, F., Tian, Y., Li, G., et al., 2025. Controls on Faulted Sub-Depression Patterns in Continental Rifted Basins: The Beier Depression, Hailar Basin, Northeastern China. Journal of Environmental & Earth Sciences. 7(5): 188–202. DOI: https://doi.org/10.30564/jees.v7i5.8543

COPYRIGHT

Copyright © 2025 by the author(s). Published by Bilingual Publishing Group. This is an open access article under the Creative Commons Attribution-NonCommercial 4.0 International (CC BY-NC 4.0) License (https://creativecommons.org/licenses/by-nc/4.0/).

1. Introduction

Intracontinental rift basins are a type of sedimentary basin primarily controlled by normal or strike-slip normal faults that develop within the upper crustal layers [1]. The basins are typically characterized by a complex interplay of numerous grabens and half-grabens, which occur in various configurations and superpositions [2, 3]. The overall structural framework and tectonic architecture of a rift basin are significantly shaped by the specific ways in which these grabens and half-grabens are combined and superimposed. Regional extension of the crust can simultaneously produce numerous half-grabens. Due to the heterogeneity of the basement, the distribution of extension laterally is uneven. In areas with less extension, there are fewer half-grabens, which may exist in isolation. In areas with greater extension, more numerous and densely packed half-grabens can connect in certain ways to form larger groups of half-grabens, thereby constituting basins or depressions. Throughout the evolution of intracontinental rift basins, variations in the regional stress field can induce the development of faults with distinct characteristics or cause a single fault to display diverse modes of activity across different stages. Normal faults with varying strike orientations and temporal activities interconnect to form an extensional fault system that governs the rifting process. This results in the complex interplay and superposition of grabens or half-grabens with different trends and temporal behaviors, ultimately leading to the formation of composite rift basins. A thorough understanding of the fundamental combination patterns of half-grabens and grabens is essential for the analysis of rift basins and has significant implications for petroleum exploration.

Situated within the eastern part of the Central Asian Orogenic Belt (CAOB), Northeastern China (NE China) and its adjacent areas are bordered by the Siberian Craton, the Western Pacific plate, and the North China Craton [4, 5]. This region contains evidence of the closure of the Paleo-Asian Ocean and the imposition and transformation of the Mongol-Okhotsk and circum-Pacific tectonic regimes during the Mesozoic [6, 7]. The Hailar Basin, positioned at the tri-national junction of Russia, Mongolia, and China in NE China (**Figure 1a**), is an extensive intracontinental rift system that mainly took shape during the late Jurassic and Cretaceous periods [8, 9]. The basin has undergone multidirectional lithospheric extension and multiple rifting events, causing the development of grabens and half-grabens with varying orientations [2, 10, 11]. Previous research has shown that other basins in NE China, such as the Erlian Basin to the west and the Songliao Basin to the southeast of the Hailar Basin, have also experienced multiphase tectonic evolution, resulting in diverse combinations of grabens and half-grabens [3, 12]. In the Erlian Basin, fault-bounded sub-depressions can be categorized into four types based on the arrangement of major faults: linear, parallel, diagonal, and interlaced. Each type comprises four compound patterns: 1) the connection of two or more half-grabens in the same direction; 2) the connection of two or more half-grabens in opposite directions; 3) the connection of a graben and a half-graben; 4) the connection of two or more grabens. Research has shown that the distribution of Early Cretaceous fault-bounded sub-depressions in the Erlian Basin was influenced by Hercynian basement zones, with depressions extending in various directions [3]. The Changling Depression Zone, one of the largest depressions in the southern part of the Songliao Basin, is a composite depression made up of multiple secondary depressions that have undergone multiple-phase tectonic evolution [12]. Based on the structural characteristics of the basin, the Changling Depression Zone can be divided into four combination types: linear, parallel, en echelon, and opposed; and two superposition types: inherited and non-inherited (coherent). The successive activity of the master boundary faults controlling the Changling composite depression zone has resulted in the vertical superposition of depressions from different periods, affecting the development of high-quality hydrocarbon source rocks. The Bohai Bay Basin also displays a similar basin structure with various combinations of grabens and half-grabens [1].

In summary, the combination patterns of different types of grabens or half-grabens in the intracontinental rift basins are primarily governed by transformations in the regional stress field and reactivation constraints imposed by pre-existing basement structures. The Beier Depression, located in the southern Middle Depression Zone of the Hailar Basin, is a composite depression composed of multiple secondary sub-depressions. It is an area where significant breakthroughs have been made in petroleum exploration within the Hailar Basin and is currently the main petroleum-producing area of the Hailar Basin. Studying the combination patterns of different types of grabens in the Beier Depression helps to

understand the combination patterns and petroleum geological characteristics of the Hailar Basin's depressions and aids in advancing knowledge of petroleum exploration in other depressions within the Hailar Basin.

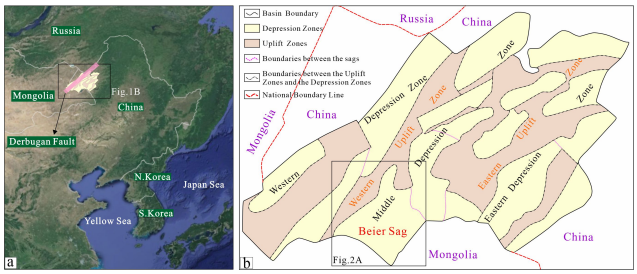


Figure 1. (**a**) Topographical map of Northeast China and its surrounding regions, illustrating the position of the Hailar Basin. (**b**) Tectonic map of the Hailar Basin, showing its subdivisions and the location of the Beier Depression.

In contrast to the basins in Northeast China, research on the combination patterns of different types of grabens or half-grabens in the Hailar Basin has been relatively limited. Do the combination patterns of different types of grabens in the basin also display similar characteristics, and what factors are responsible for this? To tackle these questions and offer novel perspectives on petroleum exploration in the Hailar Basin, this study systematically analyzed the principal fault systems, the combination patterns of faulted sub-depressions, and the underlying controlling mechanisms. The analysis was based on the most recent high-resolution 3D seismic reflection profiles that cover nearly the entire Beier Depression. The aim of this study was to elucidate the major fault systems controlling the sub-depressions, the combination patterns of different faulted sub-depressions in the Beier Depression, and the associated controlling mechanisms. The findings offer novel insights into the regional tectonic evolution of the basin, which is expected to benefit petroleum exploration in the Hailar Basin.

2. Geological Setting

2.1. Structural Framework

The Hailar-Tamtsag Basin is a northeast-trending, extensive intracontinental superimposed rift system that primarily formed during the late Jurassic and Cretaceous periods[8, 9]. Located in Northeast China and Mongolia, the basin spans approximately 400 km in length and 200 km in width[11]. The basin comprises the Hailar Basin and the Tamt Basin, with the former located in China (**Figure 1a**) and the latter in Mongolia. The formation of the Hailar-Tamtsag Basin was triggered by the closure of the Mongol-Okhotsk Ocean and the multi-phase rollback of the Paleo-Pacific slab[10, 11]. The Hailar Basin is partitioned into five major structural segments, extending from west to east: the Western Depression Zone, the Western Uplift Zone, the Central Depression Zone, the Eastern Uplift Zone, and the Eastern Depression Zone (**Figure 1b**). In these zones, the Western Depression Zone comprises three depressions, the Central Depression Zone six, and the Eastern Depression Zone seven. The Beier Depression, the principal focus of this study, is located in the southern segment of the Central Depression Zone (**Figure 1b**) and includes 13 sub-depressions (**Figure 2a**). The basin has undergone three primary developmental phases: the pre-rift stage before the Cretaceous, the syn-rift stage during the Early-Middle Cretaceous, and the post-rift stage since the Late Cretaceous. During the pre-rift stage, the basin was primarily subjected to tectonic events such as uplift, folding, and magmatism. In the pre-rift sedimentary successions, two stratigraphic units were established: the pre-rift strata and crystalline basement and the Tamulangou Formation (**Figure 2b**). Throughout the syn-rift period, the basin experienced three stages of rifting. Within the syn-rift sedimentary successions, two stratigraphic units were formed: the Tongbomiao Formation and the Nantun Formation. The Nantun Formation is separated into the Lower and Upper Nantun Formations by the T23 horizon (**Figure 2b**). During the post-rift stage, the basin was primarily subjected to subsidence, extension, and tectonic inversion events. In the post-rift sedimentary successions, three stratigraphic units were created: the Damoguaihe Formation, the Yimin Formation, and the Qingyuangang Formation (**Figure 2b**). From bottom to top, these stratigraphic units are separated by seven major horizons, namely T5, T4, T3, T23, T22, T2, and T04 (**Figure 2b**). However, the Tamulangou Formation is not present in the Beier Depression, as this sedimentary sequence had been eroded away before the onset of rifting.

2.2. Stratigraphy

The pre-rift strata and crystalline basement mainly consist of dark sandy mudstone formations, variegated sandy conglomerate formations, and volcanic rock formations that

are interbedded between them [2, 13]. The Tamulangou Formation is primarily composed of basalt, andesite, and basaltic andesite [14]. On a regional scale, the Tamulangou Formation represents the lowest stratigraphic unit of the Late Mesozoic volcanic rock sequences in the northern part of the Greater Khingan Mountains in Northeast China. It marks the beginning of extensive volcanic activity within the study area during the Late Mesozoic [14]. The Tongbomiao Formation is mainly characterized by shallow lake facies and fan delta facies sedimentary clastic rocks, which are divided into upper and lower sections. The lower section consists of variegated sandy conglomerate with thin mudstone interlayers, while the upper section is composed of gray sandstone, sandy conglomerate, and conglomerate with thin tuffaceous rock interlayers. This formation represents the first set of hydrocarbon source rocks in the study area [15]. The Nantun Formation is divided into two sections: the lower Nantun and the upper Nantun, which are generally in conformable contact. The lower Nantun Formation is composed of fan delta facies and deep lake facies sedimentary clastics, primarily characterized by gray to gray-black tuffaceous sandstone, siltstone, and interbedded mudstone. The upper Nantun Formation is made up of thick layers of dark gray to black mudstone, indicative of a deep lake sedimentary environment [13]. The Damoguaihe Formation consists of a set of semi-deep lake to braided river delta facies sediments. The lower section of the Damoguaihe Formation is marked by black mudstone and interbedded muddy siltstone and siltstone. The upper section comprises gray siltstone and sandstone with intercalated black mudstone, exhibiting rhythmic bedding. Within the basin, the Damoguaihe Formation typically transitions from a parallel unconformable contact to a conformable contact with the underlying Nantun Formation. The Yimin Formation is composed of shallow lake to fluvial facies sediments characterized by interbedded sandstone and mudstone. It is in conformable or parallel unconformable contact with the underlying Damoguaihe Formation. The Qingyuangang Formation is primarily made up of polychromatic mudstone interbedded with sandstone deposits, mainly of fluvial facies. The lower part develops gray-white conglomerate and sandy conglomerate, and it is in angular unconformity with the underlying Yimin Formation strata, with the boundary marked by the T04 seismic reflection horizon.

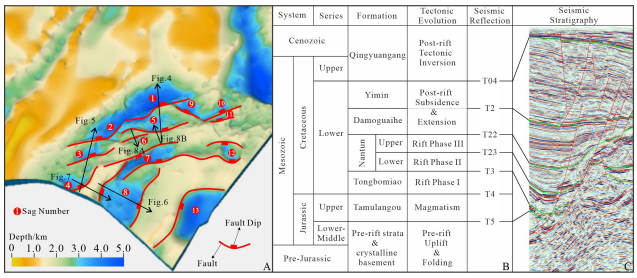


Figure 2. (**a**) Map of sub-depression divisions in the Beier Depression. (**b**) A stratigraphic column and the principal tectonic phases of the Hailar Basin. (**c**) A sample of seismic data that demonstrates the key interfaces and stratigraphic architecture.

3. Data and Methodology

3.1. Data Acquisition

This study predominantly utilizes pre-stack time-migrated high-resolution 3D reflection seismic surveys, which are integrated with numerous industrial wells. We also leverage published research outcomes and the regional and local tectonic evolution to conduct an exhaustive analysis of the major fault system that governs the sub-depressions. Furthermore, we scrutinize the combination patterns of different faulted sub-depressions in the Beier Depression, as well as the associated controlling mechanisms. All the 3D seismic surveys were collected, processed, and provided by the Exploration and Development Research Institute of Daqing Oilfield Limited Company. The Beier Depression is entirely covered by 3D reflection seismic surveys. The 3D seismic dataset features a bin spacing of 20 meters in both the inline and crossline directions. The seismic volume has sampling rates of 2 milliseconds and an average dominant frequency of 30 Hz, resulting in a vertical resolution of approximately 15 meters, given an average seismic velocity of 2000 meters per second. The vertical scale for all seismic sections in this study is based on two-way travel time.

3.2. Methodology

In this study, faults and horizons across the basin were interpreted using high-resolution seismic data processed in the Geoeast workstation. Fault identification primarily relied on seismic reflection characteristics and nearby drilling data. When an exploration well intersects a fault, the presence of fault gouge confirms the fault's existence. On seismic sections, the most evident indicator of a fault is the interrup-

tion of seismic reflectors. The number and morphological features of these reflectors may also change (e.g., increase, decrease, or show blank reflections)[16]. Interpretations were tightly constrained and calibrated using drilling data. Years of hydrocarbon exploration have yielded extensive drilling data, enabling precise fault analysis. Horizon interpretation was mainly guided by well-logging and lithology data from nearby exploratory wells, while also considering sedimentary environmental changes and reflector characteristics (such as continuity, amplitude strength, and truncation). Biostratigraphic information from foraminifera, palynology, and other petrological dating data in exploration wells was crucial for defining the chronostratigraphic framework. Six key horizons were interpreted to delineate the stratigraphy of the Beier Depression: T5, T3, T23, T22, T2, and T04. Rift-related faults throughout the Beier Depression were also interpreted and depicted by mapping fault polygons based on hanging wall and footwall cut-offs and variance slices of key seismic horizons. After interpreting faults and horizons, a 3D basement contour map featuring major rift-related faults was generated. This allowed for a clear visualization of the sub-depressions and their combination patterns.

4. Patterns of Combined Faulted Sub-Depressions in the Beier Depression and Their Characteristics

4.1. Patterns of Combined Faulted Sub-Depressions in the Beier Depression

Large numbers of normal faults often form during the early development of rift basins, with each normal fault's hanging wall developing a small-scaled half-graben. As crustal extension continued progressively, adjacent small-scaled half-grabens combine to form relatively larger structural-sedimentary units. The small-scaled faults developed in the early stage gradually link up to form long, linearly extended fault zones, which become the boundary faults controlling the structural-sedimentary units. This causes the relatively independent structural-sedimentary unit to exhibit characteristics of combined faulted sub-depressions[2, 3, 12]. As shown in **Figure 3**, according to the combination relationship of the main boundary faults controlling the grabens or half-grabens, several small half-grabens can be combined into larger scale rift patterns. These are divided into five major patterns in the Beier Depression: parallel, en echelon, face-to-face, back-to-back and S-shaped patterns.

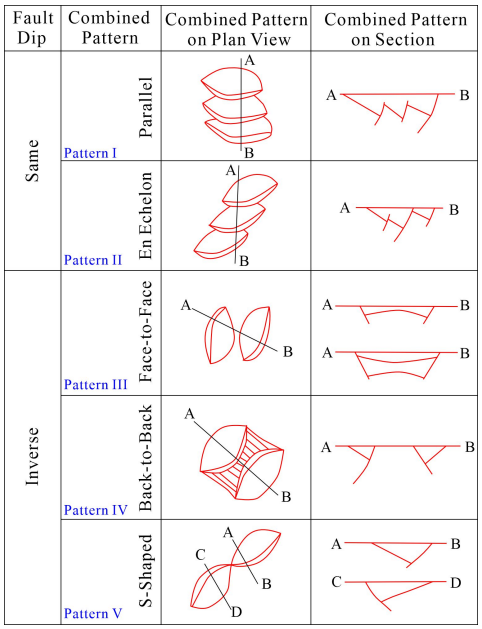


Figure 3. Summary of the combined patterns of sub-depressions in the Beier Depression.

The same directional combined patterns of the sub-depressions mainly include parallel and en echelon patterns. The parallel combined pattern (Pattern I) occurs when two or more main boundary faults with roughly the same strike and the same dip are aligned approximately parallel to each other, allowing the small half-grabens on their respective hanging walls to overlap and form a relatively unified rifted area. The en echelon combined pattern (Pattern II) involves two or more main boundary faults with essentially the same strike and the same dip arranged in an imbricated pattern, facilitating the overlap of the small half-grabens on their respective hanging walls and resulting in a relatively unified rifted area. The reverse combined patterns of the sub-depressions primarily comprise face-to-face, back-to-back, and S-shaped patterns. The face-to-face combined pattern (Pattern III) is characterized by two half-grabens in the early stage controlled by two main boundary faults with the same strike and opposite dips, distributed in parallel, with parallel sedimentation and subsidence centers within the sub-depressions. After the early stage, the two half-grabens may form a relatively unified rifted area, and that is a graben. On seismic sections, it exhibits two half-grabens with an uplifted central area in the bottom sequence unit and a graben in the later

sequence unit. The back-to-back combined pattern (Pattern IV) is defined by two small half-grabens controlled by main boundary faults with similar strikes and dips facing away from each other, distributed in parallel, with parallel sedimentation and subsidence centers within the sub-depressions. In cross-section, they manifest as an asymmetric horst structure. The S-shaped combined pattern (Pattern V) refers to two small half-grabens controlled by main boundary faults with essentially the same strike, distributed along the fault strike and connected end-to-end. However, due to the opposite fault dips, the actual sedimentation and subsidence centers of the two depressions are located parallel on both sides of the faults. In cross-section, the two sub-depressions respectively display a half-graben structure.

4.2. Characteristics of Combined Faulted Sub-Depressions on the Seismic Sections in the Beier Depression

There are 13 sub-depressions developed in the Beier Depression. The parallel combined pattern of the sub-depressions is primarily distributed in the northern Beier Depression, such as sub-depression 1 with sub-depression 5, and sub-depression 10 with sub-depression 11. The sub-depression 1 and sub-depression 5 controlled by main boundary faults with approximately NE-trending and NW-dipping, are distributed in parallel. Together, they form a relatively unified structural zone, within which sedimentation and subsidence centers are arranged in near-parallel sequences (**Figure 2a**). The sub-depression 10 and sub-depression 11 also exhibit similar characteristics on plan view. On the seismic section, it exhibits a step-like half-graben structure characterized by continuous fault steps (**Figure 4**). Moreover, the half-graben structures and stratigraphic filling patterns within the two half-grabens display similar characteristics. The en echelon combined pattern of the sub-depressions is primarily distributed in the western Beier Depression, such as tsub-depression 2, and sub-depression 3 with sub-depression 4. These three sub-depressions controlled by main boundary faults with approximately NE-trending and NW-dipping, are distributed in a right-stepping en echelon pattern, with sedimentation and subsidence centers aligned in parallel (**Figure 2a**). On the seismic section, the sub-depressions each exhibit a step-like half-graben structure characterized by continuous fault steps, and the half-graben structures and stratigraphic filling patterns within the two half-grabens display similar characteristics, similar to the parallel combined pattern of the sub-depressions (**Figure 5**). The face-to-face combined pattern of the sub-depressions is primarily distributed in the central Beier Depression, such as sub-depression 8, sub-depression 7 and sub-depression 12. These three sub-depressions are controlled separately by main boundary faults with approximately NNE-trending, NE-trending, and NEE-trending with opposite dips. In each sub-depression, the sedimentation and subsidence centers are parallel to their main boundary faults (**Figure 2a**). On the seismic section, this configuration is characterized by two half-grabens structures with an uplifted central area when the Tongbomiao Formation was developed, and then a graben structure with a subsided central area since the Nantun Formation developed (**Figure 6**). The back-to-back combined pattern of the sub-depressions is primarily distributed in the southern Beier Depression, such as sub-depression 4 with sub-depression 8, and sub-depression 8 with sub-depression 13 (**Figure 2a**). They are all separated by the uplift zones, and controlled by main boundary faults with NNE-trending and dips facing away from each other, are distributed in parallel. The sedimentation and subsidence centers within these sub-depressions are also parallel to each other. On the seismic section, this is expressed as a horst structure between the two sub-depressions (**Figure 7**). The S-shaped combined pattern of the sub-depressions is primarily distributed in the central Beier Depression, such as sub-depression 5 with sub-depression 6 (**Figure 2a**). These two sub-depressions, controlled by main boundary faults with essentially NE-trending and dips facing away from each other, are distributed along the fault strike and connected end-to-end. However, due to the opposite fault dips, the actual sedimentation and subsidence centers of the two sub-depressions are located parallel on both sides of the faults. On the seismic section, the two sub-depressions each display a half-graben structure (**Figure 8**).

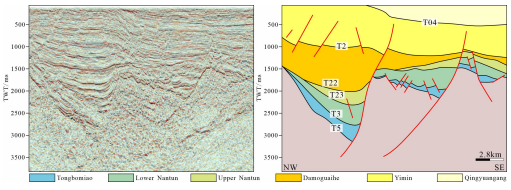


Figure 4. Seismic profile characteristics illustrate the parallel combined pattern of sub-depressions within the Beier Depression.

Note: For the location of the profile, see **Figure 2a**.

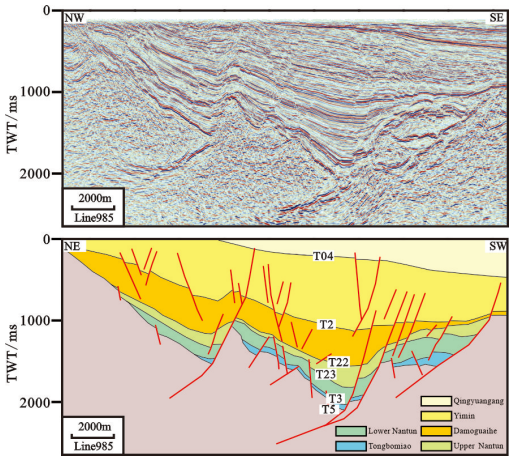


Figure 5. Seismic profile characteristics illustrate the en echelon combined pattern of sub-depressions within the Beier Depression.

Note: For the location of the profile, see **Figure 2a**.

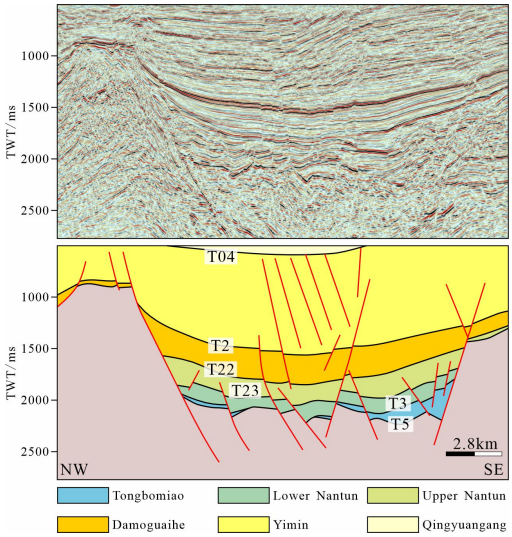


Figure 6. Seismic profile characteristics illustrate the face-to-face combined pattern of sub-depressions within the Beier Depression.

Note: For the location of the profile, see **Figure 2a**.

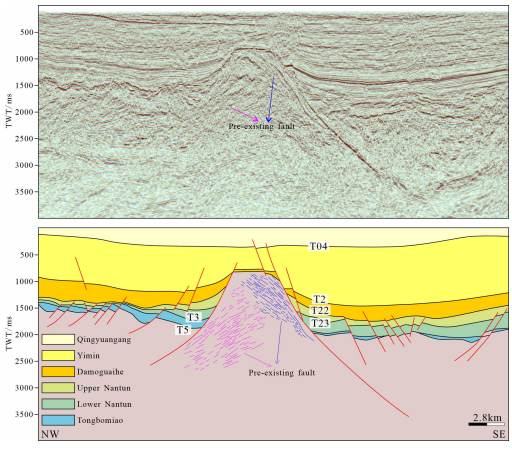


Figure 7. Seismic profile characteristics illustrate the back-to-back combined pattern of sub-depressions within the Beier Depression.

Note: Refer to **Figure 2a** for the profile's location.

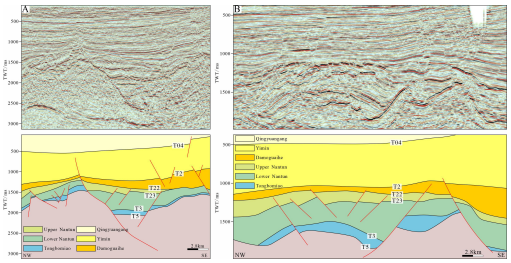


Figure 8. Seismic profile characteristics illustrate the S-shaped combined pattern of sub-depressions within the Beier Depression.

Note: Refer to **Figure 2a** for the profile's location.

5. Discussion

5.1. The Geological Development in Northeastern China Preceding the Formation of the Hailar Basin, along with the Fault Systems in the Underlying Basement

The initiation of tectonic plate separation and amalgamation often commences in regions where the lithosphere or crust harbors pre-existing weaknesses. These weaknesses typically encompass fault systems and shear zones, which are remnants of prior tectonic activities [17, 18]. The formation and evolution of rift basins are influenced not only by regional tectonic forces but also by the heterogeneity resulting from pre-existing structures such as faults and various weak zones in the basement of the rift basins [19–25]. The development of structures during rift basin formation is not random; normal faults tend to preferentially inherit these pre-existing fault surfaces or weak zones, thereby influencing the spatial distribution of the rift basin's location, shape, structure, and intensity, as well as the localization of the rifting process [24, 26–38]. Over the past two decades, the impact of pre-existing structural systems on rifting in rift basins worldwide has been extensively studied using high-precision seismic reflection data [21, 33, 36, 37, 39, 40], such as the North Sea Basin [29], the East African Rift [41], and the Northwest Shelf of Australia [42]. Studies on the Jianghan Basin inland [33], the Bohai Bay Basin in China [43, 44], the Erlian Basin [3], and the Liaohe Basin [12] in Northeast China also indicate that pre-existing structures at the base constrained the development, formation, and evolutionary process of the basin during the rifting period.

Located in the convergence of the Siberian, North China, and Pacific Plates, Northeast China marks the eastern segment of the "Central Asian Orogenic Belt" and lies

in the overlapping area of the Mongolian-Okhotsk Sea and the Pacific tectonic domain[4, 5]. The Hailar Basin is situated between the Tahe-Xiguitu Suture Zone and the Derbugan Fault Zone. As part of the Asian continent, it experienced multiple tectonic cycles before the basin formation (during the Cretaceous and earlier). Since the basin formation period (after the Mesozoic), it has been influenced by the Mongolian-Okhotsk Suture in the north and the movement of the Pacific Plate in the southeast, showing complex tectonic evolution processes[7, 45–51]. During the early to middle Jurassic, the Mongolian-Okhotsk Ocean experienced north-south subduction in both directions, closing "scissor-like" from west to east to form the northeast-trending suture zone[52–55]. After the closing event, the study area and the adjacent Northern China-Mongolia tract experienced magmatism events under the influence of the breakoff at depth of the north-dipping Mongol-Okhotsk oceanic slab[56]. With the continued collision between the Mongol-Okhotsk Oceanic Block and the Ergun Block, the study area experienced uplift and orogenic events[57]. In the late Jurassic to early Cretaceous, the Siberian Plate further squeezed southward and collided with the Ergun Block, leading to left-lateral compressional deformation along the Mongolian-Okhotsk suture zone. This resulted in the formation of northeast-trending strike-slip faults within the Ergun Block (such as the Derbugan Fault Zone)[58, 59]. Concurrently, under this left-lateral compressional deformation mechanism, a series of strike-slip associated structures were generated within the Derbugan Fault Zone, including: (**Figure 9**): 1) Northeast-east-west-trending compressional reverse faults; 2) Conjugate northeast-trending (R-shear) and northwest-trending (R'-shear) faults; 3) North-south-trending faults (T-fractures).

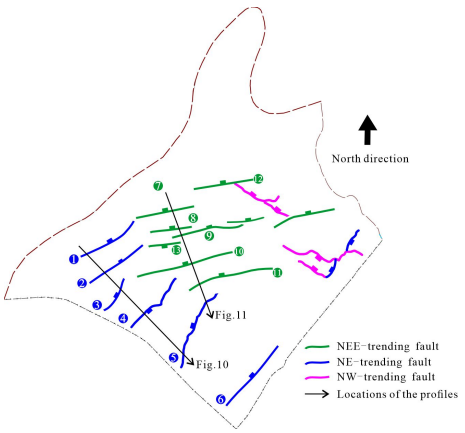


Figure 9. The arrangement of pre-existing fault systems within the basement of the Beier Depression.

The Beier Depression, part of the Hailar Basin, has a basement structure originating from the aforementioned deformation mechanisms, which include the NEE-trending reverse faults, the NE-trending R-shear faults, and the NW-trending R'-shear faults. The basement NEE-trending reverse faults are mainly found in the southwestern Beier Depression. The basement R-shear and R'-shear faults have conjugate trends. The NE-trending R-shear faults are widely developed in the central Beier Depression, while the NW-trending R'-shear faults are less common and mainly located in the northeastern part. The basement NS-trending T-faults are not developed in the Beier Depression but are mainly found in the Wuerxun Depression to the north. These basement faults with various trends, acting as pre-existing structures, undergo multiple deformations when the tectonic regime changes later, thus exhibiting different characteristics. The NEE-trending and NE-trending fault systems are the dominant pre-existing fault systems controlling the Beier Depression's structure. The basement NE-trending R-shear faults are characterized by high-amplitude, continuous strong reflections on seismic sections (**Figure 10**). These faults typically have a listric shape, with most dipping towards the NW and some towards the SE (**Figure 10**). In the central uplift's basement, fault-plane-like reflections can be observed (**Figure 7**). The basement faults on the far left and right have been reactivated, controlling the formation of Sub-depressions 4 and 8, respectively. These two faults are pre-existing NE-trending faults. Thus, the reflective layer in the central uplift zone, resembling fault planes, should be NE-trending pre-existing faults with different dips. In the sedimentary layers, the primary fault plane is relatively planar, converging towards shear zones in the basement (**Figure 10**). Almost all these faults offset the Tongbomiao, Nantun, Damoguaihe, and Yimin Formations, extending to the basement and the T04 interface. The NEE-trending fault systems are characterized by medium-amplitude, moderately continuous strong reflections in the sedimentary layers on seismic sections (**Figure 11**). In the basement, one major NEE-trending fault shows high-amplitude, continuous strong reflections, with other NEE-trending faults converging towards it. These faults typically have a listric shape, all dipping towards the NW (**Figure 11**). Almost all these faults offset the Tongbomiao and Nantun Formations, with three offsetting the Damoguaihe and Yimin Formations. All extend

to the basement, with only one reaching the T04 interface. Since the early Early Cretaceous, the Hailar Basin entered the rifting stage, and these faults were successively reactivated under different stress fields.

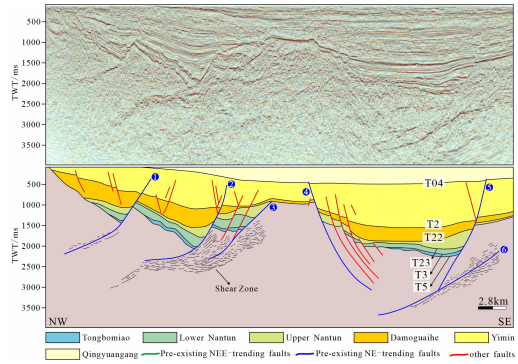


Figure 10. The seismic profile features depict the pre-existing northeast-trending fault systems in the Beier Depression.

Note: The location of the profile is shown in **Figure 9**.

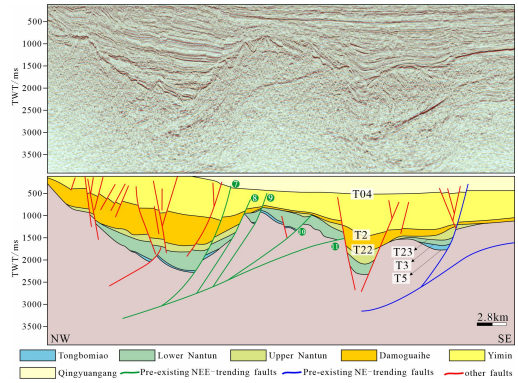


Figure 11. The seismic profile characteristics illustrate the pre-existing NEE-trending fault systems in the Beier Depression.

Note: Refer to **Figure 9** for the profile's location.

5.2. The Tectonic Evolution in Northeast China since the Initiation of the Hailar Basin's Formation

Since the Early Cretaceous, tectonic movements from various periods have been successively superimposed on the basement structure, resulting in multiple phases of tectonic deformation in the Hailar Basin [6, 46, 49, 56, 60–65]. As previously mentioned, the Mongolian-Okhotsk Ocean closed "scissor-like" from west to east to form the northeast-trending suture zone, followed by the breakoff of the slab and subsequent uplift events from the early to late Jurassic [52–57]. In the late Jurassic to early Cretaceous, the Siberian Plate further moved southward and collided with the Ergun Block, causing left-lateral compressional deformation along the Mongolian-Okhotsk suture zone and forming northeast-trending strike-slip faults within the Ergun Block. In the early Early Cretaceous, this regional strike-slip movement led to the lithospheric delamination of the Mongol-Okhotsk orogenic belt, triggering regional extensional tectonics in the study area and resulting in the formation of fault-controlled rift basins bounded by boundary faults and the deposition of the Tongbomiao Formation [6]. During this period, the direction of regional extensional stress was NNW-SSE. As the collision between the Siberian Block and the Ergun Block continued, along with the onset of subduction of the eastern Paleo-Pacific Plate, the Hailar Basin remained under an extensional stress regime oriented in the NNW-SSE direction, leading to the deposition of the Lower Nantun Formation. With the continued horizontal subduction of the Paleo-Pacific Plate, slab delamination of the Pacific Plate occurred, triggering another episode of rifting in the Hailar Basin and depositing the Upper Nantun Formation [6, 46, 60, 61]. The direction of regional extensional stress during this period was NW-SE, indicating a counterclockwise rotation compared to the previous period. At the end of the Nantun Formation deposition, the subduction direction of the Paleo-Pacific Plate changed from SSW to NW, causing approximately S-N directed compression in the study area, tilting and eroding the strata, and the basin experienced fold-type inversion [55, 66]. Around 125 Ma later, the retreat of the Paleo-Pacific Plate subduction led to near E-W directed extension in the study area, causing extensional or oblique extensional deformation of faults and depositing the Damoguaihe and Yimin Formations, marking the basin's subsidence period [6, 67]. Around 110 Ma, a reorganization of the Paleo-Pacific Plate resulted in low-angle, rapid westward subduction, causing near E-W directed regional compression in the study area, intrabasinal transpressional inversion, and deposition of the Qingyuangang Formation during the basin's inversion period [6, 68]. In summary, the Hailar Basin experienced multiple episodes of regional subsidence and extension events induced by regional strike-slip activities and thickened lithospheric delamination (during the Tongbomiao Formation deposition), Paleo-Pacific Plate subduction slab delamination (during the Nantun Formation deposition), and the return of the Paleo-Pacific Plate (during the Damoguaihe-Yimin Formation deposition). Additionally, changes in the subduction direction of the Paleo-Pacific Plate (at the end of the Nantun Formation) and the reorganization

of the Paleo-Pacific Plate (Andean-type active margin) led to multiple episodes of regional tectonic compression events due to low-angle subduction of the Paleo-Pacific Plate.

5.3. Factors Controlling the Patterns of Combined Faulted Sub-Depressions in the Beier Depression

Pre-existing structures can generally be divided into three categories: lithospheric-scale pre-existing structures and weak zones, basin-scale pre-existing structural systems, and small-scale individual pre-existing faults[21, 28, 69–72]. Lithospheric-scale pre-existing structures and weak zones (including large-scale lithospheric shear zones and plate suture boundaries formed by tectonic activities) typically determine the development location and rift axis orientation of rift basins due to their position and distribution[28, 69, 71, 73–76]. Basin-scale pre-existing structural systems mainly consist of pre-existing faults and folds that develop within the upper crust. Rift basins influenced by pre-existing structures typically exhibit irregular basin morphologies, segmentation of rifts, special combinations of graben and half-graben units, and multi-directional fault systems[22, 41, 72, 77–79]. The reactivation of small-scale individual pre-existing faults in later stages significantly impacts the geometric characteristics and kinematic processes of normal faults[21, 70]. The pre-existing fault system developed in the basement of the Hailar Basin mainly belongs to the basin-scale pre-existing structural system, which primarily controls the basin morphology, special combinations of graben and half-graben units, and so on. As discussed in Section 5.2, during the periods when the Tongbomiao and the Lower Nantun Formations were deposited, the Hailar Basin was under an NNW-SSE extensional stress field. Under such a stress field, pre-existing fault systems with NEE-trending are more likely to become reactivated. During the period when the Upper Nantun Formation was deposited, the Hailar Basin was under an NW-SE extensional stress field. In such a stress field, the pre-existing basement fault systems with NE-trending are more likely to be reactivated, as the orientation of these faults is more favorably aligned with the direction of the stress field. Observations based on the depositional characteristics of strata in seismic profiles also support this viewpoint (**Figures 10** and **11**). That is, the deposition of the Tongbomiao Formation and the Lower Nantun Formation in the Hailar Basin was primarily controlled by the reactivation of pre-existing faults trending in the NEE direction within the basement, while the deposition of the Upper Nantun Formation was mainly controlled by the reactivation of pre-existing faults trending in the NE direction within the basement. In the Beier Depression, the thickness of the Tongbomiao Formation is very thin, indicating that the rifting was relatively weak during this period (**Figures 10** and **11**). The thickness of the Lower and Upper Nantun Formations are much thicker, indicating a relatively much more intensive rifting process in the study area.

In regions where sedimentary strata are influenced by pre-existing NEE-trending faults, the paleo-throw of the Lower Nantun Formation is typically greater than that of the Upper Nantun Formation. This is attributed to the higher activity of NEE-trending faults during the deposition of the Lower Nantun Formation, resulting in a larger vertical offset between the hanging wall and footwall. In contrast, in areas controlled by NE-trending pre-existing faults, the paleo-throw of the Lower Nantun Formation is smaller than that of the Upper Nantun Formation, indicating increased activity of NE-trending faults during the Upper Nantun depositional period. For example, with NE-trending faults numbered 1 and 2 (**Figure 10**), the thickness of the Lower Nantun Formation is consistent between the hanging wall and footwall, while the hanging wall's Upper Nantun Formation is significantly thicker than the footwall's, suggesting enhanced fault activity during the Upper Nantun period. Moreover, for faults numbered 3, 4, and 5 (**Figure 10**), which are NE-trending pre-existing faults, the Upper Nantun Formation is noticeably thicker than the Lower Nantun Formation, further indicating the reactivation of NE-trending faults during the Upper Nantun period. By comparison, faults numbered 7 to 11 (**Figure 11**), which are NEE-trending pre-existing faults, show a clear predominance in the thickness of the Lower Nantun Formation over the Upper Nantun Formation, with a greater paleo-throw for the Lower Nantun Formation. This suggests that these NEE-trending faults were the primary active fault systems during the Lower Nantun depositional period. These observations all indicate that during the rifting process in the Hailar Basin, the NEE-trending pre-existing fault system was activated first, followed by the NE-trending fault system. This sequence of fault activation has affected the depositional patterns and the stratigraphic thickness dis-

tribution within the basin, reflecting the evolving tectonic regime throughout the depositional history of the basin.

The varying orientations, dips, arrangements, and activation sequences of the pre-existing fault systems together shaped the developmental features and spatial distribution of the sub-depressions within the Beier Depression. These elements influenced the diverse patterns of combined faulted sub-depressions in the Beier Depression. Faults with similar strikes and dips arranged in an En echelon pattern (faults numbered 1, 2, and 3) control the En echelon combination of sub-depressions. Faults with similar strikes and dips arranged approximately parallel to each other (faults numbered 9 and 12) control the Parallel combination of sub-depressions. Faults with the same strike and opposite dips (face-to-face), distributed in parallel (faults numbered 4 and 5), control the face-to-face combination of sub-depressions. Meanwhile, faults with similar strikes and dips facing away from each other, distributed in parallel (faults numbered 3 and 4), control the back-to-back combination of sub-depressions. Faults with the same strike, distributed along the fault strike and connected end-to-end (faults numbered 9 and 13), control the S-shaped combination of sub-depressions.

6. Conclusions

A comprehensive study focusing on the major fault system, the combination patterns of faulted sub-depressions, and the underlying controlling mechanisms was conducted. This study was based on the most recent high-resolution 3D seismic reflection profiles that nearly cover the entire Beier Depression. The principal findings are as follows:

1. Three groups of pre-existing fault systems were identified in the basement of the Beier Depression. These are the NEE-EW-trending fault systems, the NE-trending fault systems, and the NW-trending fault systems.
2. The NEE-EW-trending fault systems were distributed in the central part of the Beier Depression and primarily controlled the sedimentary filling of the Tongbomiao and the Lower Nantun Formations. The NE-trending fault systems were distributed in the southwestern part of the Beier Depression and primarily controlled the sedimentary filling of the Upper Nantun Formations. The NW-trending fault systems were distributed rarely in the Beier Depression.
3. Five kinds of combined patterns of the sub-depressions were developed in the Beier Depression, and they are the parallel, en echelon, face-to-face, back-to-back, and S-shaped combined patterns.
4. The parallel combined pattern of sub-depressions was mainly controlled by the faults with essentially the same strike and the same dip arranged approximately parallel to each other. The en echelon combined pattern of sub-depressions was mainly controlled by the faults with essentially the same strike and the same dip arranged in en echelon pattern. Face-to-face combined pattern of sub-depressions was mainly controlled by the faults with the same strike and opposite dips (face-to-face), distributed in parallel. The back-to-back combined pattern of sub-depressions was mainly controlled by the faults with the same strike and dips facing away from each other, distributed in parallel. The faults with the same strike, distributed along the fault strike and connected end-to-end, control the S-shaped combined pattern of sub-depressions.

In summary, the five kinds of combined patterns of the sub-depressions developed in the Beier Depression are predominantly governed by the reorientation of the regional stress field and the reactivation constraints imposed by pre-existing basement structures. The hydrocarbon exploration implications of these five distinct graben/half-depression configurations for basin-scale resource assessment will constitute a key focus for future research priorities.

Author Contributions

Conceptualization, G.L. and Y.W.; methodology, H.L.; software, Y.Z; validation, M.L., Y.T. and G.L.; formal analysis, F.C.; resources, Y.T.; data curation, Y.W.; writing—original draft preparation, F.C.; writing—review and editing, G.L.; visualization, Y.Z.; supervision, H.L; project administration, Y.T.; funding acquisition, F.C. All authors have read and agreed to the published version of the manuscript.

Funding

This research was supported by the Major National Science and Technology Programs of China (No. 2016E-0202,

No. QGYQZYPJ2022-1).

Institutional Review Board Statement

Not applicable.

Informed Consent Statement

Not applicable.

Data Availability Statement

The original data in this study is unavailable due to privacy.

Acknowledgments

The authors wish to express their gratitude to the Editor and the anonymous reviewers for their efforts and valuable suggestions that have greatly improved the manuscript. Appreciation is extended to the Exploration and Development Research Institute of PetroChina Daqing Oilfield Company Limited for supplying the seismic reflection data used in this study.

Conflicts of Interest

The authors declare no commercial conflict of interest

References

[1] Min, A, Na, N., Zhang, F., et al., 2013. Early Cretaceous provenance change in the southern Hailar Basin, northeastern China and its implication for basin evolution. Cretaceous Research. 40, 21–42.

[2] Agostini, A., Corti, G., Zeoli, A., et al., 2009. Evolution, pattern, and partitioning of deformation during oblique continental rifting: Inferences from lithospheric-scale centrifuge models. Geochemistry, Geophysics, Geosystems. 10(11), 154–163.

[3] Bird, P.C., Cartwright, J.A., Davies, T.L., 2015. Basement reactivation in the development of rift basins; an example of reactivated Caledonide structures in the West Orkney Basin. Journal of the Geological Society. 172(1), 77–85.

[4] Bramham, E.K., Wright, T.J., Paton, D.A., et al., 2021. A new model for the growth of normal faults developed above pre-existing structures. Geology. 49(5), 587–591.

[5] Brune, S., Autin, J., 2013. The rift to break-up evolution of the Gulf of Aden: Insights from 3D numerical lithospheric-scale modelling. Tectonophysics. 607, 65–79.

[6] Brune, S., Williams, S.E., Müller, R.D., 2018. Oblique rifting: The rule, not the exception. Solid Earth. 9(5), 1187–1206.

[7] Cheng, Y., Wu, Z., Su, W., et al., 2023. Basement structures exert a crucial influence on the structural configuration of later rift development: Insights from the Shanan and Chengbei depression, Bohai Bay Basin. Marine and Petroleum Geology. 153, 106272.

[8] Cogné, J.P., Kravchinsky, V.A., Halim, N., et al., 2005. Late Jurassic-Early Cretaceous closure of the Mongol-Okhotsk Ocean demonstrated by new Mesozoic palaeomagnetic results from the Trans-Baikal area (SE Siberia). Geophysical Journal International. 163(2), 813–832.

[9] Collanega, L., Siuda, K., Jackson, C.A.L., et al., 2019. Normal fault growth influenced by basement fabrics: The importance of preferential nucleation from pre-existing structures. Basin Research. 31(4), 659–687.

[10] Corti, G., Calignano, E., Petit, C., et al., 2011. Controls of lithospheric structure and plate kinematics on rift architecture and evolution: An experimental modeling of the Baikal rift. Tectonics. 30(3).

[11] Corti, G., Cioni, R., Franceschini, Z., et al., 2019. Aborted propagation of the Ethiopian rift caused by linkage with the Kenyan rift. Nature Communications. 10(1), 1309.

[12] Deng, H., McClay, K., 2019. Development of extensional fault and fold system: Insights from 3D seismic interpretation of the Enderby Terrace, NW Shelf of Australia. Marine and Petroleum Geology. 104, 11–28.

[13] Dong, S., Zhang, Y., Li, H., et al., 2018. The Yanshan orogeny and late Mesozoic multi-plate convergence in East Asia-Commemorating 90th years of the "Yanshan Orogeny". Science China Earth Sciences. 61, 1888–1909.

[14] Fazlikhani, H., Fossen, H., Gawthorpe, R.L., et al., 2017. Basement structure and its influence on the structural configuration of the northern North Sea Rift. Tectonics. 36(6), 1151–1177.

[15] Gouiza, M., Naliboff, J., 2021. Rheological inheritance controls the formation of segmented rifted margins in cratonic lithosphere. Nature Communications. 12(1), 4653.

[16] Gu, C., Zhu, G., Zhang, S., et al., 2017. Cenozoic evolution of the Yilan-Yitong Graben in NE China: An example of graben formation controlled by pre-existing structures. Journal of Asian Earth Sciences. 146, 168–184.

[17] Guan, W., Huang, L., Liu, C., et al., 2023. Interactions between preexisting structures and rift faults: Implications for basin geometry in the northern South China

Sea. Basin Research. 1–27.

[18] Heron, P.J., Peace, A.L., McCaffrey, K.J.W., et al., 2019. Segmentation of rifts through structural inheritance; creation of the Davis Strait. Tectonics. 38(7), 2411–2430.

[19] Henstra, G.A., Kristensen, T.B., Rotevatn, A., et al., 2019. How do pre-existing normal faults influence rift geometry? A comparison of adjacent basins with contrasting underlying structure on the Lofoten Margin, Norway. Basin Research. 31(6), 1083–1097.

[20] Ji, Z., Meng, Q., Wan, C., et al., 2019a. Generation of late Mesozoic felsic volcanic rocks in the Hailar Basin, northeastern China in response to overprinting of multiple tectonic regimes. Scientific Reports. 9(1), 15854.

[21] Ji, Z., Meng, Q.A., Wan, C.B., et al., 2019b. Geodynamic evolution of flat-slab subduction of Paleo-Pacific Plate: Constraints from Jurassic adakitic lavas in the Hailar Basin, NE China. Tectonics. 38(12), 4301–4319.

[22] Ji, Z., Wan, C.B., Meng, Q.A., et al., 2020. Chronostratigraphic framework of late Mesozoic terrestrial strata in the Hailar-Tamtsag Basin, Northeast China, and its geodynamic implication. Geological Journal. 55(7), 5197–5215.

[23] Jia, J., Tao, S., Fang, X., et al., 2021. Deep Jurassic volcano-sedimentary succession, reservoir-seal assemblage and their exploration significance in Northeast China: A case study of Jurassic in the Hailar Basin. Acta Geologica Sinica. 95(2), 377–395.

[24] Keranen, K., Klemperer, S.L., 2008. Discontinuous and diachronous evolution of the Main Ethiopian Rift: Implications for development of continental rifts. Earth and Planetary Science Letters. 265(1–2), 96–111.

[25] Kolawole, F., Firkins, M., Al-Wahaibi, T.S., et al., 2021. Rift interaction zones and the stages of rift linkage in active segmented continental rift systems. Basin Research. 33(6), 2984–3020.

[26] Kravchinsky, V.A., Jean-Pascal, C., Harbert, W.P., et al., 2002. Evolution of the Mongol-Okhotsk ocean as constrained by new palaeomagnetic data from the Mongol-Okhotsk suture zone, Siberia. Geophysical Journal International. 148 (1), 34–57.

[27] Li, G., Mei, L., Ye, Q., et al., 2023. Post-rift faulting controlled by different geodynamics in the Pearl River Mouth Basin, northern South China Sea margin. Earth-Science Reviews. 237, 104311.

[28] Li, S.C., Liu, Z.H., Xu, Z.Y., et al., 2015. Age and tectonic setting of volcanic rocks of the Tamulangou Formation in the Great Xing'an Range, NE China. Journal of Asian Earth Sciences. 113, 471–480.

[29] Liu, S., Fu, X., Wang, Y., et al., 2020. Depression evolution in muti-phase rifts: Case study on the Paleogene of Qikou Depression. Chinese Journal of Geology. 55(1), 81–92.

[30] Liu, Z.H., Wan, C.B., Ren, Y.G., et al., 2006. Geological features and the rule of oil and gas accumulation of Wurxun-Beier Subbasin in Hailaer Basin. Journal of Jilin University. 36, 527–534.

[31] Luo, J., Sun, Y., Wang, Y., et al., 2021. Cenozoic tectonic evolution of the eastern Liaodong Bay sub-basin, Bohai Bay basin, eastern China-Constraints from seismic data. Marine and Petroleum Geology. 134, 105346.

[32] Manatschal, G., Lavier, L., Chenin, P., 2015. The role of inheritance in structuring hyperextended rift systems: Some considerations based on observations and numerical modeling. Gondwana Research. 27(1), 140–164.

[33] McClay, K.R., White, M.J., 1995. Analogue modelling of orthogonal and oblique rifting. Marine and Petroleum Geology. 12, 137–151.

[34] Meng, E., Xu, W.L., Yang, D.B., et al., 2011. Zircon U-Pb chronology, geochemistry of Mesozoic volcanic rocks from the Lingquan basin in Manzhouli area, and its tectonic implications. Acta Petrologica Sinica. 27(4), 1209–1226.

[35] Meng, Q.R., 2003. What drove late Mesozoic extension of northern China-Mongolia tract? Tectonophysics. 369, 155–174.

[36] Meng, Q., Zhu, D., Chen, J., et al., 2012. Styles of complex faulted depressions in rifting basin and its significance for petroleum geology: An example from Hailar-Tamtsag Early Cretaceous Basin. Earth Science Frontiers. 19(5), 76–85.

[37] Meng, Q.A., Wan, C.B., Zhu, D.F., 2013. Age assignment and geological significance of the 'Budate Group' in the Hailar Basin. Science China: Earth Sciences. 56, 970–979.

[38] Morley, C.K., 2014. The widespread occurrence of low-angle normal faults in a rift setting: Review of examples from Thailand, and implications for their origin and evolution. Earth-Science Reviews. 133, 18–42.

[39] Muirhead, J.D., Kattenhorn, S.A., 2018. Activation of preexisting transverse structures in an evolving magmatic rift in East Africa. Journal of Structural Geology. 106, 1–18.

[40] Odepressioniede, E.E., Rotevatn, A., Gawthorpe, R., et al., 2020. Pre-existing intrabasement shear zones influence growth and geometry of noncolinear normal faults, western Utsira High–Heimdal Terrace, North Sea. Journal of Structural Geology. 130, 103908.

[41] Parfenov, L.M., Popeko, L.I., Tomurtogoo, O., 2001. Problems of tectonics of the Mongol-Okhotsk orogenic belt. Geology of the Pacific Ocean. 16, 797–830.

[42] Phillips, T.B., Fazlikhani, H., Gawthorpe, R.L., et al., 2019. The influence of structural inheritance and multiphase extension on rift development, the northern North Sea. Tectonics. 38(12), 4099–4126.

[43] Pichel, L.M., Antunes, A.F., Fossen, H., et al., 2023. The interplay between basement fabric, rifting, syn-rift folding, and inversion in the Rio do Peixe Basin, NE Brazil. Basin Research. 35(1), 61–85.

[44] Jian, Ren., Dingyou, L.Y.U., Xingpeng, C.H.E.N., et al., 2019. Oblique extension of pre-existing structures and its control on oil accumulation in eastern Bohai Sea. Petroleum Exploration and Development. 46(3), 553–564.

[45] Rotevatn, A., Kristensen, T.B., Ksienzyk, A.K., et al., 2018. Structural inheritance and rapid rift-length establishment in a multiphase rift: The East Greenland rift system and its Caledonian orogenic ancestry. Tectonics. 37(6), 1858–1875.

[46] Rotevatn, A., Jackson, C.A.L., Tvedt, A.B., et al., 2019. How do normal faults grow?. Journal of Structural Geology. 125, 174–184.

[47] Salazar-Mora, C.A., Huismans, R.S., Fossen, H., et al., 2018. The Wilson cycle and effects of tectonic structural inheritance on rifted passive margin formation. Tectonics. 37(9), 3085–3101.

[48] Samsu, A., Micklethwaite, S., Williams, J.N., et al., 2023. Structural inheritance in amagmatic rift basins: Manifestations and mechanisms for how pre-existing structures influence rift-related faults. Earth-Science Reviews. 246, 104568.

[49] Scholz, C.A., Shillington, D.J., Wright, L.J.M., et al., 2020. Intrarift fault fabric, segmentation, and basin evolution of the Lake Malawi (Nyasa) Rift, East Africa. Geosphere. 16(5), 1293–1311.

[50] Shaban, S.N., Kolawole, F., Scholz, C.A., 2023. The deep basin and underlying basement structure of the Tanganyika Rift. Tectonics. 42(7), e2022TC007726.

[51] Song, J., Liu, Z., Wang, C., et al., 2019. Multistage structural deformations of a superimposed basin system and its tectonic response to regional geological evolution: A case study from the Late Jurassic-Early Cretaceous Tanan depression, Hailar-Tamtsag basin. Marine and Petroleum Geology. 110, 1–20.

[52] Sorokin, A.A., Kudryashov, N.M., Sorokin, A.P., 2005. Late Paleozoic Urusha Magmatic Complex in the southern framing of the Mongolia-Okhotsk Belt (Amur Region): Age and geodynamic setting. Petrology. 13, 596–610.

[53] Sun, W., Zhang, L., 2022. Preface: Pacific plate subduction and the Yanshanian movement in Eastern China. Journal of Earth Science. 33(3), 541–543.

[54] Tang, J., Xu, W.L., Wang, F., et al., 2015. Geochronology, geochemistry, and deformation history of Late Jurassic-Early Cretaceous intrusive rocks in the Erguna Massif, NE China: constraints on the Late Mesozoic tectonic evolution of the Mongol-Okhotsk orogenic belt. Tectonophysics. 658, 91–110.

[55] Tong, H., Koyi, H., Huang, S., et al., 2014. The effect of multiple pre-existing weaknesses on formation and evolution of faults in extended sandbox models. Tectonophysics. 626, 197–212.

[56] Walsh, J.J., Nicol, A., Childs, C., 2002. An alternative model for the growth of faults. Journal of Structural Geology. 24(11), 1669–1675.

[57] Wan, C.B., 2006. Cretaceous Palynological Flora in Hailar Basin [PhD thesis]. Changchun, China: Jilin University. pp. 1–209.

[58] Wang, D., Li, P., Shan, X., et al., 2019. Seismic evidence for nappes in basins west of the Da Hinggan Mountains. Chinese Journal of Geophysics. 62(3), 1129–1138.

[59] Wang, D., Zhang, X., Yang, L., et al., 2022. Influence of pre-existing faults on Cenozoic structures in the Chengbei depression and the Wuhaozhuang area, Bohai Bay Basin, East China. Marine and Petroleum Geology. 138, 105539.

[60] Wang, T., Guo, L., Zhang, L., et al., 2015. Timing and evolution of Jurassic-Cretaceous granitoid magmatisms in the Mongol-Okhotsk belt and adjacent areas, NE Asia: Implications for transition from contractional crustal thickening to extensional thinning and geodynamic settings. Journal of Asian Earth Sciences. 97, 365–392.

[61] Wang, Y., Lu, Y., Fu, G., et al., 2014. Structure features and natural gas enrichment regularity in Changling fault depression groups. Oil Geophysical Prospecting. 49(6), 1204–1212.

[62] Wu, L., Mei, L., Paton, D.A., et al., 2020. Basement structures have crucial influence on rift development: Insights from the Jianghan Basin, Central China. Tectonics. 39(2), e2019TC005671.

[63] Wu, L., Shen, C., Paton, D A., et al., 2023. A rift-scale view at strain partitioning during multiphase rifting: Insights from the Hailar Basin, northeast Asia. Basin Research. 00, 1–24.

[64] Wu, L., Shen, C., Paton, D.A., et al., 2024. Rift segmentation caused by reactivation of multiple basement structure systems: Evidence from the Hailar-Tamtsag Rift, Northeast Asia. Basin Research. 36, e12841.

[65] Xu, M.J., Xu, W.L., Meng, E., 2011. LA-ICP-MS zircon U-Pb chronology and geochemistry of Mesozoic volcanic rocks from the Shanghulin-Xiangyang basin in Ergun area, northeastern Inner Mongolia. Geological Bulletin of China. 30, 1321–1338.

[66] Yang, G., Yin, H., Gan, J., et al., 2022. Explaining structural difference between the eastern and western zones of the Qiongdongnan Basin, northern South China Sea: Insights from scaled physical models. Tectonics. 41(2), e2021TC006899.

[67] Yang, Y., Guo, Z., Song, C., et al., 2015. A short-lived but significant Mongol-Okhotsk collisional orogeny in latest Jurassic-earliest Cretaceous. Gondwana Research. 28(3), 1096–1116.

[68] Yi, Z., Meert, J.G., 2020. A closure of the Mongol-Okhotsk Ocean by the Middle Jurassic: Reconciliation of paleomagnetic and geological evidence. Geophysical Research Letters. 47(15), e2020GL088235.

[69] Zhang, F., Dilek, Y., Chen, H., et al., 2017. Structural

architecture and stratigraphic record of Late Mesozoic sedimentary basins in NE China: Tectonic archives of the Late Cretaceous continental margin evolution in East Asia. Earth-Science Reviews. 171, 598–620.

[70] Zhang, J.H., Ge, W.C., Wu, F.Y., 2006. Mesozoic bimodal volcanic suite in Zhalantun of the Da Hinggan Range and its geological significance: Zircon U-Pb age and Hf isotopic constraints. Acta Geologica Sinica-English Edition. 80, 58–69.

[71] Zhang, K., Deng, B., Zhang, F., et al., 2016. Determination of early stage of Early Cretaceous compressive event in Hailar Basin, NE China, and its tectonic significance. Earth Science-Journal of China University of Geosciences. 41(7), 1141–1155.

[72] Zhang, Y., Dong, S., 2019. East Asia multi-plate convergence in Late Mesozoic and the development of continental tectonic systems. Journal of Geomechanics. 25(5), 613–641.

[73] Zhang, Y., Qiu, E., Dong, S., et al., 2022. Late Mesozoic intracontinental deformation and magmatism in North and NE China in response to multi-plate convergence in NE Asia: An overview and new view. Tectonophysics. 835, 229377.

[74] Zhao, P., Xu, B., Chen, Y., 2023. Evolution and final closure of the Mongol-Okhotsk Ocean. Science China Earth Sciences. 66(11), 2497–2513.

[75] Zhao, X.Z., Jin, F.M., Qi, J.F., et al., 2015. The structural types and petroleum geological significance of Early Cretaceous complex faulted depression in Erlian Basin. Natural Gas Geoscience. 26(7), 1289–1298.

[76] Zheng, C.Q., Zhou, J.B., Jin, W., 2009. Geochronology in the north segment of the Derbugan fault zone, Great Xing'an Range, NE China. Acta Petrologica Sinica. 25, 1989–2000.

[77] Zhou, J., Li, L., 2017. The Mesozoic accretionary complex in Northeast China: Evidence for the accretion history of Paleo-Pacific subduction. Journal of Asian Earth Sciences. 145, 91–100.

[78] Zhou, Y., Ji, Y.L., Pigott, J.D., et al., 2014. Tectonostratigraphy of Lower Cretaceous Tanan sub-basin, Tamtdepression Basin, Mongolia: Sequence architecture, depositional systems and controls on sediment infill. Marine and Petroleum Geology 49, 176–202.

[79] Zwaan, F., Schreurs, G., 2017. How oblique extension and structural inheritance influence rift segment interaction: Insights from 4D analog models. Interpretation. 5(1), SD119–SD138.